Biochemical and genetic evidence supports Fyv6 as a second-step splicing factor in *Saccharomyces cerevisiae*

KARLI A. LIPINSKI,[1,3] KATHERINE A. SENN,[2,3] NATALIE J. ZEPS,[2] and AARON A. HOSKINS[1,2]

[1]Department of Chemistry, University of Wisconsin-Madison, Madison, Wisconsin 53706, USA
[2]Department of Biochemistry, University of Wisconsin-Madison, Madison, Wisconsin 53706, USA

ABSTRACT

Precursor mRNA (pre-mRNA) splicing is an essential process for gene expression in eukaryotes catalyzed by the spliceosome in two transesterification steps. The spliceosome is a large, highly dynamic complex composed of five small nuclear RNAs and dozens of proteins, some of which are needed throughout the splicing reaction while others only act during specific stages. The human protein FAM192A was recently proposed to be a splicing factor that functions during the second transesterification step, exon ligation, based on analysis of cryo-electron microscopy (cryo-EM) density. It was also proposed that Fyv6 might be the *Saccharomyces cerevisiae* functional and structural homolog of FAM192A; however, no biochemical or genetic data has been reported to support this hypothesis. Herein, we show that Fyv6 is a splicing factor and acts during exon ligation. Deletion of *FYV6* results in genetic interactions with the essential splicing factors Prp8, Prp16, and Prp22 and decreases splicing in vivo of reporter genes harboring intron substitutions that limit the rate of exon ligation. When splicing is assayed in vitro, whole-cell extracts lacking Fyv6 accumulate first-step products and exhibit a defect in exon ligation. Moreover, loss of Fyv6 causes a change in 3′ splice site (SS) selection in both a reporter gene and the endogenous *SUS1* transcript in vivo. Together, these data suggest that Fyv6 is a component of the yeast spliceosome that influences 3′ SS usage and the potential homolog of human FAM192A.

Keywords: Fyv6; FAM192A; spliceosome; yeast; RNA splicing

INTRODUCTION

The removal of introns from precursor mRNA (pre-mRNA) molecules is carried out by the spliceosome, a large macromolecular complex made up of five small nuclear RNAs (snRNAs) and dozens of proteins which assemble de novo on each pre-mRNA substrate. Splicing consists of two, stepwise transesterification reactions in which the 5′ splice site (5′ SS; the boundary between the 5′ exon and the intron) is first cleaved by the formation of a lariat intron (first step) and then the intron is released concomitant with exon ligation by attack of the 5′ exon at the 3′ SS (second step). Spliceosome composition changes dramatically throughout the course of splicing due to the sequential arrivals and departures of different components as well as large-scale conformational changes (Plaschka et al. 2019). This results in the formation of several intermediate complexes with distinct architectures during the reaction, many of which have now been visualized by cryo-electron microscopy (cryo-EM) (Plaschka et al. 2019). Cleavage of the 5′ SS is completed during the transition from the spliceosome B* to the C complex, and exon ligation occurs during the transition between the C* and P (product) complexes. While some components of the spliceosome remain part of the machine throughout the reaction, others transiently associate, dissociate, or rearrange to interact with the catalytic site only at specific times. Just prior to 5′ SS cleavage, the first-step factors (Cwc25, Isy1, and Yju2) function to juxtapose the 5′ SS and branch site (BS) (Villa and Guthrie 2005; Liu et al. 2007a; Chiu et al. 2009; Wan et al. 2019; Wilkinson et al. 2021). Cwc25 and Isy1 are then released after 5′ SS cleavage, and second-step factors bind (Slu7, Prp18) or are repositioned (Prp17) to facilitate exon ligation (James et al. 2002; Ohrt et al. 2013; Fica et al. 2017; Yan et al. 2017; Plaschka et al. 2019). Proper progression through splicing requires the coordinated association and dissociation of these first- and second-step factors with the active site and these transitions are enabled, in part, by ATP-dependent DExD/H-box helicases. The ATPase Prp16 promotes rearrangement of the

[3]These authors contributed equally to this work.
Corresponding author: ahoskins@wisc.edu
Article is online at http://www.rnajournal.org/cgi/doi/10.1261/rna.079607.123.

spliceosome active site and splicing factor release between the first and second step of splicing (Schwer and Guthrie 1992; Semlow et al. 2016), while Prp22 promotes release of the mRNA product from the spliceosome after exon ligation (Wagner et al. 1998; Schwer 2008).

Recently, a putative new second-step factor (FAM192A or PIP30) was identified for the human spliceosome. The protein was found by fitting unassigned density present in cryo-EM maps of spliceosomes transitioning between conformations competent for the first or second steps (Zhan et al. 2022). Depletion of FAM192A from human nuclear extracts reduced in vitro splicing, but adding purified protein back did not restore this activity, potentially due to the simultaneous depletion of other, unidentified splicing factors (Zhan et al. 2022). Consequently, its role in splicing is still poorly defined.

Interestingly, Zhan et al. also identified a potential FAM192A homolog, Fyv6 (function required for yeast viability 6), in *Saccharomyces cerevisiae* (hereafter, yeast) despite having <20% sequence identity (Fig. 1A). (It should be noted, however, that this level of sequence identity is similar to that between yeast and human homologs of the other second-step factors Slu7 and Prp18.) The predicted AlphaFold structure of Fyv6 (Jumper et al. 2021) was able to be modeled as three α-helices into unassigned EM density from yeast C* spliceosome complexes previously

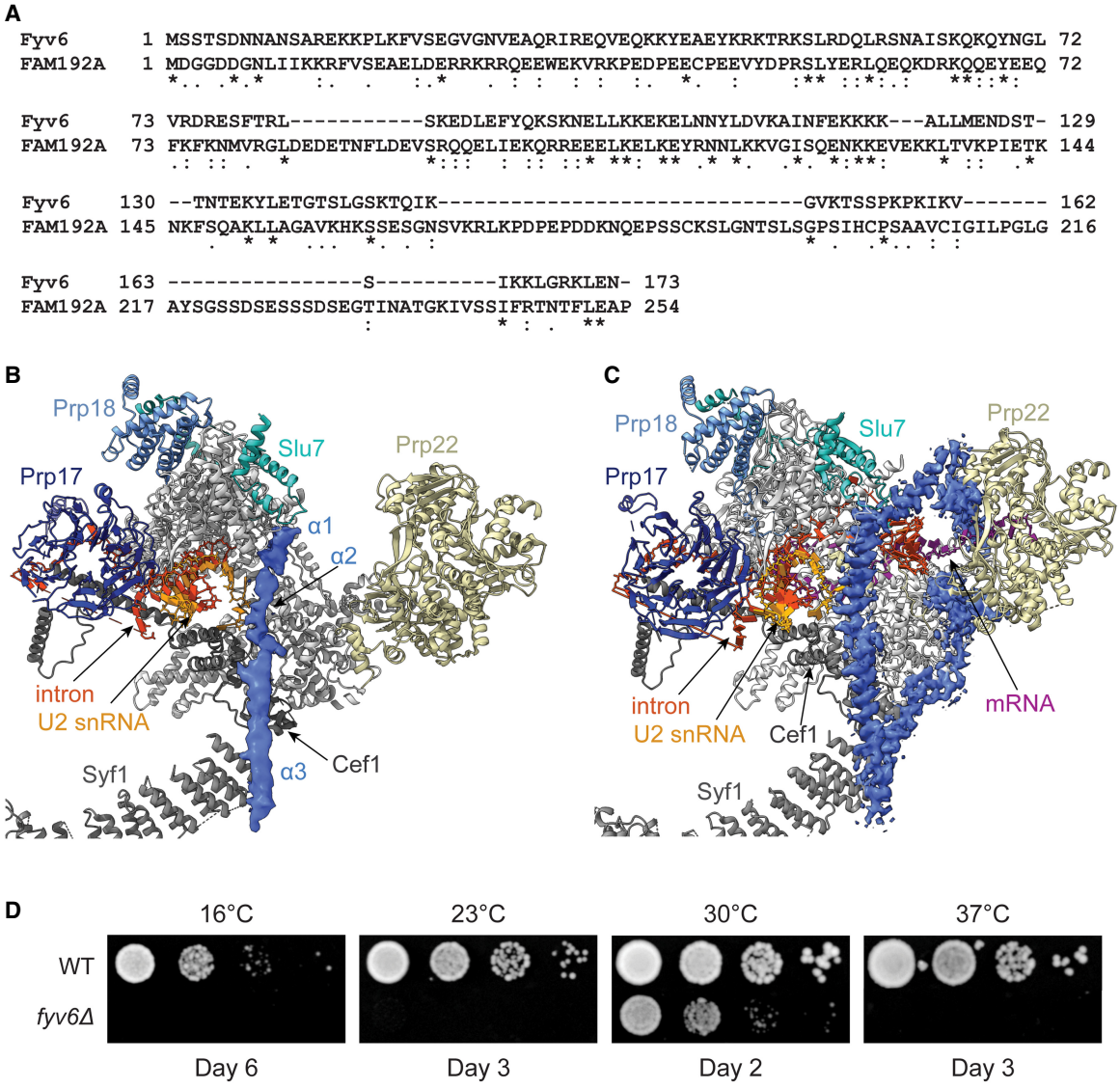

FIGURE 1. Sequence alignment of Fyv6 with FAM192 and unassigned EM density in yeast spliceosome structures. (*A*) Sequence-based alignment of *S. cerevisiae* Fyv6 and human FAM192A using EMBOSS Needle (Needleman and Wunsch 1970). (*B*,*C*) Superposition of the atomic models for the spliceosome C* (panel *B*, 5MQ0) and P (panel *C*, 6BK8) complexes with the unassigned EM density shown in blue spacefill. The three putative Fyv6 α helices identified by Zhan and coworkers are annotated next to the corresponding EM density in panel *B*. Images were prepared using ChimeraX (Pettersen et al. 2021). (*D*) Impact of *fyv6Δ* on yeast growth at various temperatures. Plates were imaged on the days shown.

labeled as unknown protein X (Fig. 1B; α1–3 labeled as in Zhan et al. 2022). Prior to this work, Fyv6 had been detected by mass spectrometry analysis of purified B^{act} and C complex spliceosomes (Fabrizio et al. 2009; Warkocki et al. 2009) as well as postulated to be responsible for unassigned density in a cryo-EM structure of a yeast P complex spliceosome (referred to as UNK in that structure, Fig. 1C; Liu et al. 2017). In both the C* and P complex spliceosomes, the unassigned EM density is located in a position that could significantly impact splicing chemistry: in C* the density contacts core splicing factors Cef1, Syf1, and Prp8, while in P complex it contacts these factors in addition to the lariat intron, Slu7, and Prp22 (Fig. 1; Supplemental Fig. S1). The unassigned densities in the yeast cryo-EM structures occupy positions on the spliceosome that are very similar to the position of FAM192A in the human pre-C* structures, which contacts the human homologs of these splicing factors (Supplemental Movie S1). Together, the combined cryo-EM and mass spectrometry data hint at Fyv6 functioning during splicing; however, no genetic or biochemical evidence for this has been reported.

Fyv6 is a poorly studied and nonessential yeast protein originally identified in a screen for mutants sensitive to K1 killer toxin (Pagé et al. 2003). Since identification, Fyv6 has appeared in genetic screens for mutants with sensitivity to heat (Auesukaree et al. 2009), calcineurin inhibitor FK506 (Viladevall et al. 2004), and changes to cell size (Maitra et al. 2019). Fyv6 is localized to the nucleus and has previously been proposed to play a role in nonhomologous end joining, but little is known about its function or interacting partners (Wilson 2002; Huh et al. 2003). Here, we studied the function of Fyv6 during splicing by probing genetic interactions between Fyv6 and the splicing factors Prp8, Prp16, and Prp22. In addition, we assayed splicing in vivo and in vitro by deleting *FYV6* and showed that its loss inhibits exon ligation. Finally, we used both a reporter gene and an endogenous transcript to examine how the loss of *FYV6* impacts 3′ SS selection. Together, these data are consistent with Fyv6 functioning as a second-step splicing factor in yeast.

RESULTS

Genetic interactions between Fyv6 and Prp8 first or second-step alleles

To examine a potential role for Fyv6 in splicing, we deleted *FYV6* from the yeast genome, confirmed the deletion by PCR (Supplemental Fig. S2), and assayed for genetic interactions with known splicing factors. While *FYV6* is nonessential for yeast viability, its deletion does cause a slow growth defect at 30°C and both cold and temperature sensitivity (*cs* and *ts*) phenotypes at other temperatures (Fig. 1D). We first tested for genetic interactions with the essential spliceosome component Prp8. Prp8 is a central protein in the spliceosome that scaffolds the active site RNAs and can impact equilibria between the intron branching and exon ligation reactions through structural rearrangement (Query and Konarska 2004; Fica and Nagai 2017). As such, multiple alleles of Prp8 stabilize the spliceosome in either the first- or second-step conformation at the expense of the other state (Fig. 2A; Umen and Guthrie 1995a; Schneider et al. 2004; Query and Konarska 2004; Liu et al. 2007b). Moreover, alleles of second-step factors Prp18 and Slu7 (*prp18-1*, *slu7-1*, *slu7-ccss*) are synthetically lethal with a first-step allele of Prp8 (*prp8-101* or $Prp8^{E1960K}$) (Umen and Guthrie 1995b), presumably since both alleles work in concert to promote the first step or inhibit proper progression to the second step. Since Fyv6, like Slu7 and Prp18, is predicted to interact with Prp8 (Supplemental Fig. S1), we expected that genetic interactions should occur between Fyv6 and Prp8 if the former is also involved in splicing.

Plasmid shuffle of a gene expressing $Prp8^{E1960K}$ into a *fyv6Δ* strain resulted in synthetic lethality even at the normally permissive temperature of 30°C (Fig. 2B). Synthetic lethality was also observed for another first-step allele of Prp8, *prp8-R1753K* (Fig. 2B). In contrast, when we shuffled in a second-step allele, *prp8-161* ($Prp8^{P986T}$), we observed suppression of the growth defect caused by *fyv6Δ* at both 30°C and 37°C (Fig. 2B,C). When the P986T and R1753K mutations were combined, synthetic lethality was still observed with *fyv6Δ* (Fig. 2B). These results are consistent with Fyv6 acting to promote the second step of splicing and its deletion, *fyv6Δ*, promoting the first step. Combining *fyv6Δ* with a first-step Prp8 allele can be synthetically lethal due to failure to properly transition to the second step, while combining *fyv6Δ* with a second-step allele may improve yeast growth by facilitating proper first-step/second-step equilibrium.

Genetic interactions between Fyv6 and Prp16 or Prp22

Prp8 first and second-step alleles, as well as first and second-step alleles in U6 snRNA and Cef1, can also genetically interact with mutants of the Prp16 or Prp22 ATPases that promote the first to second-step transition or exit out of the second step by product release, respectively (Fig. 2A; Query and Konarska 2006, 2012; Eysmont et al. 2019). Based on these observations, we next tested genetic interactions between *fyv6Δ* and Prp16 or Prp22 mutants that may slow these conformational changes. $Prp16^{R686I}$ likely slows the first to second-step transition, leads to a *cs* phenotype at 16°C (Hotz and Schwer 1998), and is synthetically lethal with first-step Prp8 alleles (Query and Konarska 2006). A yeast strain with *fyv6Δ* plus $Prp16^{R686I}$ exacerbates the cold sensitivity, resulting in almost no growth at 16°C and reduced growth at 23°C compared to strains with either allele alone (Fig. 2D). The combination of $Prp16^{R686I}$

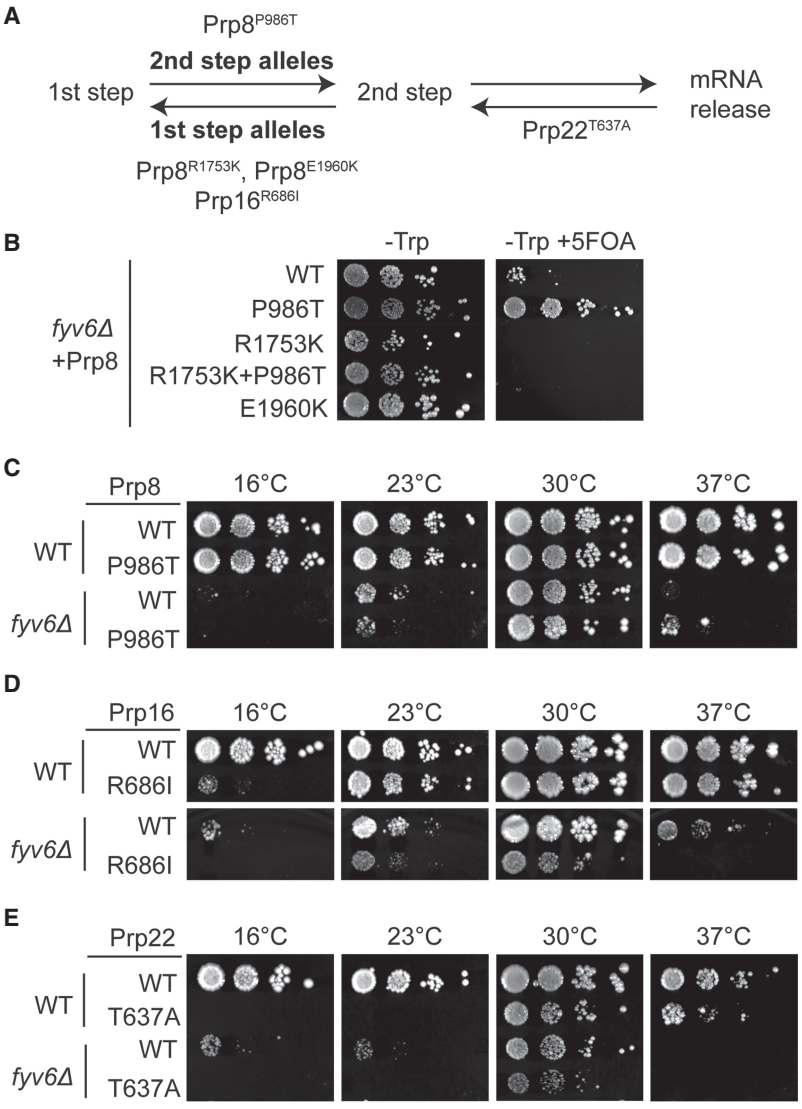

FIGURE 2. Genetic interactions between Fyv6 and Prp8, Prp16, or Prp22. (*A*) Diagram of how Prp8, Prp16, and Prp22 alleles impact the first and second steps of splicing. (*B*) Alleles of Prp8 were combined with *fyv6Δ* in Prp8 shuffle strains and grown on −Trp or −Trp + 5-FOA plates. Yeast growth was imaged after 3 d at 30°C. (*C*) Prp8^{P986T}/*fyv6Δ* strains were tested for suppression or exacerbation of temperature-dependent growth phenotypes. (*D*,*E*) Alleles of Prp16 and Prp22 were combined with *fyv6Δ* and tested for suppression or exacerbation of temperature-dependent growth phenotypes. For panels *C*–*E*, yeast were plated on YPD and imaged after 3 (30°C), 4 (23°C and 37°C), or 10 (16°C) days.

with *fyv6Δ* also results in reduced growth at 30°C and is synthetic lethal at 37°C. Both *fyv6Δ* and first-step Prp8 alleles interact negatively with the Prp16^{R686I} ATPase.

The Prp22^{T637A} mutant uncouples ATP hydrolysis from RNA unwinding (Schwer and Meszaros 2000), likely perturbing the transition out of the second-step conformation and product release. Prp22^{T637A} is also a *cs* allele and does not grow at 16°C or 23°C (Fig. 2E; Schwer and Meszaros 2000) and is synthetically lethal with second-step alleles of Cef1 (Query and Konarska 2012). When Prp22^{T637A} and *fyv6Δ* were combined, we did not observe any suppression of the *cs* phenotype of Prp22^{T637A} or the *cs*/*ts* phenotype of *fyv6Δ* (Fig. 2E). Prp22^{T637A}/*fyv6Δ* yeast were viable at 30°C but grew more slowly than strains containing only a single allele. The genetic interactions with Prp22^{T637A} are difficult to interpret as one could expect destabilization of the second-step conformation by *fyv6Δ* to suppress defects in mRNA release from Prp22^{T637A}. Alternatively, slowed product release by Prp22^{T637A} could favor a longer lifetime of the exon ligation conformation and suppression of defects caused by *fyv6Δ*. The genetic and potential physical interactions between Fyv6 and Prp22 need further study to disentangle how the proteins are influencing these steps collaboratively or not.

Impact of *fyv6Δ* on yeast growth using the ACT1–CUP1 splicing reporter assay

If Fyv6 is a component of the splicing machinery as the genetic interactions suggest, we would also predict changes in in vivo splicing in the absence of the protein. To test this, we used the ACT1–CUP1 reporter assay in which changes in the splicing of the reporter pre-mRNA (Fig. 3A) confer proportional changes in the copper tolerance of a sensitized yeast strain with increased splicing efficiency leading to growth at higher copper concentrations (Lesser and Guthrie 1993). Since yeast lacking Fvy6 grow more slowly than WT even under optimal growth conditions (Fig. 1D, for example) we scored WT yeast growth on Cu^{2+}-containing plates after 48 h but *fyv6Δ* yeast were scored after 72 h. Consistent with the slow growth and with a function of Fyv6 during splicing, we observed slightly reduced copper tolerance for even the WT ACT1–CUP1 reporter in the *fyv6Δ* strain (Fig. 3B,C).

We also tested several ACT1–CUP1 reporters containing substitutions in the 5′ (U2A, A3C, and A3U) or 3′ SS (UuG and gAG) or the BS (A258U, BSG, and BSC) (Fig. 3A) to determine if loss of Fyv6 is especially detrimental or beneficial to introns with nonconsensus sequences. This set of reporters includes those that are limiting for the first step (A258U), those that accumulate lariat intermediates due to being limiting for the second step (U2A, A3C, BSG,

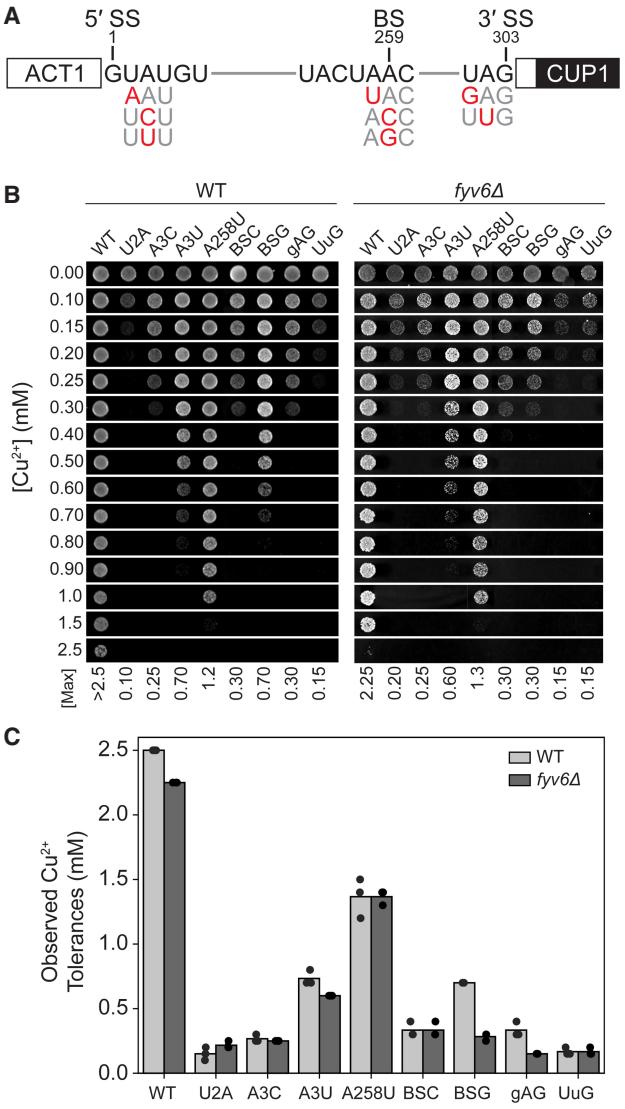

FIGURE 3. Impact of *FYV6* deletion on yeast copper tolerance using the ACT1–CUP1 assay. (*A*) Schematic of the WT ACT1–CUP1 reporter along with intronic substitutions. (*B*) Images of representative yeast growth on copper-containing media shown after 48 (WT) or 72 h (*fyv6Δ*) for strains containing the indicated ACT1–CUP1 reporters. (*C*) Maximum copper tolerances observed for each strain for $N = 3$ replicates (dots). Bars represent the average values.

UuG, and gAG), and those that are limiting for both steps of splicing (BSC) (Lesser and Guthrie 1993; Liu et al. 2007b). Previous work has shown that first-step alleles of Prp8 result in reduced copper tolerance and fewer ligated mRNA products with the U2A, A3C, BSC, BSG, UuG, and gAG reporters and that second-step alleles of Prp8 or Cef1 improve copper tolerance of yeast with the U2A, BSC, BSG, UuG, and gAG reporters (Liu et al. 2007b; Query and Konarska 2012). We would predict, therefore, that if *fyv6Δ* is a first-step allele we should see reduced copper tolerance of reporters limiting for the second step of splicing, similar to those in Prp8.

When we tested this prediction, we found that copper tolerance was similar between WT and *fyv6Δ* yeast containing reporters with the A3C, UuG, A258U, and BSC substitutions. However, strains containing A3U, BSG, and gAG reporters exhibited less tolerance to copper than WT (Fig. 3B,C), suggesting poorer splicing of pre-mRNAs with these substitutions. We conclude that loss of Fyv6 results in a subset of changes in copper tolerance akin to first-step alleles of Prp8 and is consistent with Fyv6 supporting the second step when present.

While the strongest effects in the ACT1–CUP1 assay support the involvement of Fyv6 in the second step, it should be noted that we also observed a slight increase in copper tolerance in the presence of U2A (Fig. 3B,C). The U2A reporter is a 5′ SS mutant but is not limiting for the first step as it can readily accumulate lariat intermediates that can be discarded from the spliceosome (Liu et al. 2007b). This suggests that it is defective for the transition to the second step or the second step itself. As described in the preceding paragraph, second-step alleles of Prp8 also increase the copper tolerance of yeast with the U2A reporter (Liu et al. 2007b). This could mean that *fyv6Δ* can, at least in this case of U2A, provide some support for the second step as well.

First-step products accumulate in the absence of Fyv6 in vitro

We next tested if Fyv6 plays a role in exon ligation using in vitro splicing assays with whole-cell extracts (WCEs) made from either WT or *fyv6Δ* yeast. Splicing extracts made from the same yeast strains used in the ACT1–CUP1 assays show accumulation of first-step products and decreased second-step efficiency in the absence of Fyv6 (Fig. 4). Interestingly, this effect was less pronounced when the BJ2168 protease-deficient yeast strain commonly used to prepare WCEs was used (Supplemental Fig. S3). This strain also displayed less cold sensitivity at 23°C (close to the temperature at which in vitro splicing assays are conducted) than the *cup1Δ* strains when *FYV6* was deleted (Supplemental Fig. S3A). This suggests that the strength of some *fyv6Δ* phenotypes may be strain dependent.

Loss of Fyv6 changes 3′ SS selection

Since both Prp18 and Slu7 can change 3′ SS selection (Frank and Guthrie 1992; Kawashima et al. 2009, 2014) and Slu7 contacts the unassigned density attributed to Fyv6 (Fig. 1B,C), we tested whether or not loss of Fyv6 can also change splicing outcomes. We utilized an ACT1–CUP1 reporter containing an additional, alternative 3′ SS proximal to the BS which results in a frameshift when used instead of the distal 3′ SS (Fig. 5A). Previous studies with this reporter showed that use of the proximal 3′ SS greatly increases in the presence of the *slu7-1* allele with

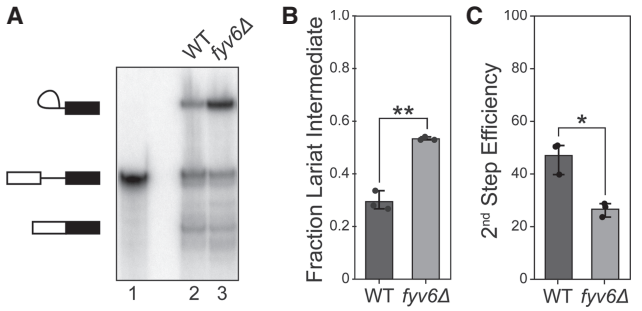

FIGURE 4. Accumulation of splicing intermediates occurs in the absence of Fyv6 in in vitro splicing assays. (*A*) Products of the first and second steps after incubation of a radioactively labeled RP51A pre-mRNA (lane *1*) in WCE from *cup1Δ* strains (yAAH0434 and yAAH3353, Supplemental Table 1) for 45 min (lanes *2*,*3*). Quantitation of (*B*) lariat intermediates or (*C*) Second-step splicing efficiency from three replicates. Statistical significance was determined by unpaired Welch's two-tailed *t*-test ($P = 0.006415$ and 0.01788 for fraction of lariat intermediate and second-step efficiency, respectively). The fraction of the lariat intermediate represents the fraction of that species relative to the substrate and all splicing products while the second-step efficiency represents the fraction of mRNA relative to the sum of first- and second-step products (lariat intermediate plus mRNA). Details for calculations can be found in the Materials and Methods.

an ~20-fold change in the ratio of mRNAs produced using the proximal versus distal sites (Frank and Guthrie 1992). Indeed, when this reporter was used, we observed the largest differences in copper tolerance (Fig. 5B). To confirm that this change in survival was due to a change in 3′ SS usage and use of the proximal SS, we isolated RNAs from the yeast strains and quantified SS usage by primer extension. These results showed an increase in the use of the proximal SS and an approximately fivefold increase in the ratio of mRNAs produced using the proximal versus distal sites (Fig. 5C, D). Moreover, these data suggest that Fyv6, like Slu7, helps to enforce a preference for BS distal 3′ SS. However, one limitation of our studies is that we have not mapped the BS used in the absence of Fyv6 and cannot completely exclude the possibility of an upstream, cryptic BS in the ACT1 intron (Kao et al. 2021) driving usage of the proximal 3′ SS. Nonetheless, we believe that this is less likely than a change in the second-step reaction itself given our in vitro data (Fig. 4).

Finally, we examined if the loss of Fyv6 impacts the splicing of endogenous yeast transcripts in vivo. Given its sensitivity to perturbations in the splicing machinery (Hossain et al. 2009; Cuenca-Bono et al. 2011; Hossain et al. 2011), we examined *SUS1* splicing—one of the rare genes in yeast with two introns. We performed RT-PCR on RNA extracted from strains that either contained (WT) or lacked *FYV6* and additionally were *upf1Δ* to prevent nonsense-mediated decay (NMD) of unspliced or alternatively spliced transcripts (Sayani et al. 2008). In the case of the WT *upf1Δ* yeast, we observed products for unspliced, partially spliced (one of two introns removed), and fully spliced mRNA. The *fyv6Δ* strain has these same products present in the WT strain as well as a product that is slightly larger than the fully spliced mRNA (Fig. 6A). This larger product was also seen upon RT-PCR of *SUS1* in the BJ2168 *fyv6Δ* strain (Supplemental Fig. S3E). The appearance of the new band was the biggest change in splicing of *SUS1* upon *FYV6* deletion (Fig. 6B). We sequenced this product and determined that it results from the use of an alternative 3′ SS in the first intron of *SUS1* that, to our knowledge,

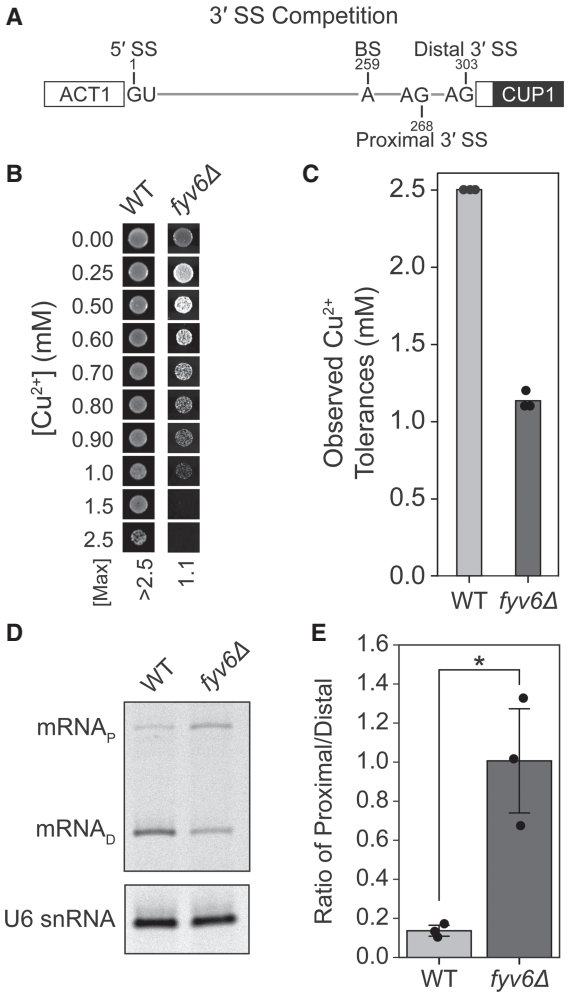

FIGURE 5. Loss of Fyv6 changes 3′ SS selection in yeast. (*A*) Schematic of the 3′ SS competition reporter (3′ SS comp) showing relative locations of the proximal and distal sites. (*B*) Images of representative yeast growth on copper-containing media shown after 48 (WT) or 72 h (*fyv6Δ*) for strains containing the 3′ SS comp ACT1–CUP1 reporter. (*C*) Maximum copper tolerances observed for each strain for $N = 3$ replicates (dots). Bars represent the average values. (*D*) Representative primer extension analysis of mRNAs generated by yeast using the distal ($mRNA_D$) or proximal ($mRNA_P$) 3′ SS in the presence (WT) or absence of Fyv6 (*fyv6Δ*). U6 snRNA was analyzed as a loading control. (*E*) Quantification of the primer extension results from $N = 3$ replicates (dots) expressed as a ratio of $mRNA_P/mRNA_D$. Bars represent the average of the replicates ±SD. Means between the two experimental groups were compared with an unpaired Welch's two-tailed *t*-test ($P = 0.04262$).

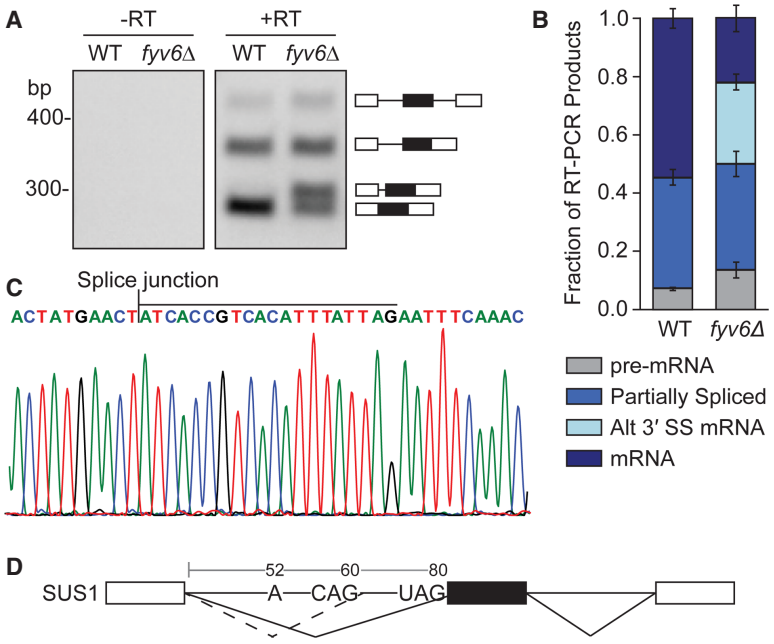

FIGURE 6. Loss of Fyv6 results in the use of an alternative 3′ SS in *SUS1*. (*A*) Representative gel image of RT-PCR of *SUS1* in strains with (WT) and without (*fyv6Δ*) Fyv6 in a *upf1Δ* background. (+RT reactions contain reverse transcriptase; −RT control reactions do not contain reverse transcriptase). (*B*) Quantification of band intensities of each isoform as a fraction of the total *SUS1* product in a lane. The bars indicate the average of three experiments with standard deviation. (*C*) Portion of the Sanger sequencing chromatogram of the *SUS1* splice variant identified as an RT-PCR product in the *fyv6Δ* strain. The bar *above* the nucleotides indicates those from intron 1 included in the splice variant due to the use of an alternative 3′ SS. (*D*) Diagram of the *SUS1* gene structure with the BS adenosine and the two, alternative 3′ SS of intron 1 indicated. The numbering of the nucleotides begins at the first nucleotide of intron 1. The newly identified 3′ SS is at position 60.

has not previously been reported (Fig. 6C,D). In this isoform, the last twenty nucleotides of intron 1 are retained, and an intronic CAG located proximal to the BS is used as the alternate 3′ SS. This new splice site is only 8 nt downstream from the BS adenosine (Fig. 6D). It is possible that this transcript is normally degraded by NMD since it includes a premature termination codon 35 amino acids into the coding sequence, and the corresponding isoform was less prevalent by RT-PCR from the Upf1-containing BJ2168 strain (Supplemental Fig. S3E).

DISCUSSION

Together, the genetic and biochemical data presented here as well as the mass spectrometry and cryo-EM work of others, indicate that yeast Fyv6 is a second-step splicing factor and likely is a component of the spliceosome. Our results do not, however, confirm that the unassigned EM density present in yeast C* and P complex spliceosome cryo-EM maps is due to Fyv6. Further work will be needed to verify that this is indeed the case either through obtaining higher resolution cryo-EM data or experimental approaches that probe protein–protein interactions to map the Fyv6 binding site.

The results we obtained for the deletion of *FYV6* are similar to those reported for perturbations of other second-step splicing factors. Different alleles of Fyv6, Slu7, or Prp18 result in synthetic lethality with first-step alleles of Prp8 (Umen and Guthrie 1995b). Like Fyv6, the second-step factors Slu7, Prp18, and Prp22 also affect 3′ SS choice (Frank and Guthrie 1992; Crotti et al. 2007; Kawashima et al. 2014; Semlow et al. 2016). Interestingly, in strains lacking Fyv6, 3′ SS that were within nine nucleotides of the BS were used more frequently in ACT1–CUP1 and *SUS1* (Figs. 5, 6). This resembles observations made with Slu7, which is necessary for the use of any splice sites that are >9 nt downstream from the BS (Brys and Schwer 1996). Structurally, Slu7 is positioned within the spliceosome in a way that suggests that it could guide distal 3′ SS into the correct location (Fica et al. 2017; Wilkinson et al. 2017). In addition, Prp22 is important for splicing when the 3′ SS is >20 nt away from the BS (Schwer and Gross 1998). In the human spliceosome, FAM192A is proximal to Prp22, Slu7, and the intron (Supplemental Movie S1). This suggests that, as a potential FAM192 homolog and in agreement with the unassigned density in yeast spliceosomes (Fig. 1B,C), Fyv6 could also impact the second-step spliceosome conformation and/or positioning of the intron either directly through contacts with the intron or via interactions with Slu7 and Prp22.

Many outstanding questions remain about Fyv6 function. We do not know when Fyv6 associates or dissociates from the spliceosome, whether it can function at stages other than exon ligation, or the structural mechanism behind its influence on 3′ SS usage. Finally, since it seems likely that Fyv6 is the functional yeast homolog of human FAM192A in terms of pre-mRNA splicing, it will be worth investigating if other functions of FAM192A/Fyv6 are conserved in yeast. FAM192A also associates with the 20S proteasome via interaction with PA28γ, a 20S proteasome regulator, for ubiquitin-independent protein degradation within the nucleus (Jonik-Nowak et al. 2018). While yeast lack an apparent homolog for PA28γ (Jonik-Nowak et al. 2018), it may be interesting to determine if Fyv6 is involved in protein degradation and if there are any Fyv6-dependent links between proteostasis and pre-mRNA splicing.

MATERIALS AND METHODS

Yeast strains and plasmids used in this study are described in Supplemental Tables S1, S2. Yeast transformation, plasmid shuffling/5-FOA selection, and growth were carried out using standard techniques and media (Sikorski and Boeke 1991; Treco and Lundblad 1993).

Network analysis of potential Fyv6 interactions

Protein–protein and protein–RNA interactions found in the atomic model for the P complex spliceosome (6BK8) were identified using LouiseNET, and the resulting nodes and edges were plotted as an undirected network model using GEPHI, as previously described (Bastian et al. 2009; Kaur et al. 2022).

Deletion strain creation

The *FYV6* and *UPF1* genes were deleted through replacement with a hygromycin or kanamycin resistance cassette, respectively, by homologous recombination (see Supplemental Table S1; Goldstein and McCusker 1999). Gene deletion was confirmed by genomic DNA extraction from the strains and PCR amplification of the corresponding genomic locus. Primers for FYV6 were Fyv6-check-fwd 5′-TGGATCGAACACAGGACCTC-3′ and Fyv6-check-rev 5′-GTGGAACGAGCAATCAATGTGATC-3′. Primers for UPF1 were Upf1-check-up 5′-CAGCCAACAAACGTTGAAGATTTCATC-3′ and Upf1-check-down 5′-TTGCAGCGCTCATTTCACGGTTGAGC-3′.

ACT1–CUP1 copper tolerance assays

Yeast strains expressing ACT1–CUP1 reporters were grown to stationary phase in −Leu DO media to maintain selection for plasmids, diluted to $OD_{600} = 0.5$ in 10% (v/v) glycerol, and spotted onto −Leu DO plates containing 0–2.5 mM $CuSO_4$ (Lesser and Guthrie 1993; Carrocci et al. 2018). Plates were scored and imaged after 48 h of growth at 30°C for WT strains, and after 72 h of growth at 30°C for *fyv6Δ* strains due to differential growth between strains.

Growth assays

For temperature-dependent growth assays, yeast strains were grown overnight to stationary phase in YPD media, diluted to $OD_{600} = 0.5$ in 10% (v/v) glycerol, and stamped onto YPD plates. The plates were incubated at 16°C, 23°C, 30°C, or 37°C for the number of days indicated in each figure before imaging.

For growth assays in the presence of 5-FOA, yeast strains were grown overnight to stationary phase in −Trp DO media, diluted to $OD_{600} = 0.5$ in 10% (v/v) glycerol, and stamped onto −Trp and −Trp +5-FOA plates. The plates were incubated at 30°C for 3 d before imaging.

Primer extension

Cell cultures were inoculated from stationary phase saturated cultures grown overnight in −Leu DO media. The cultures were then grown until $OD_{600} = 0.6–0.8$, and 10 OD_{600} units were collected by centrifugation. Total RNA was isolated from yeast, and contaminating DNA was depleted using the MasterPure Yeast RNA Purification Kit (Epicentre) protocol, with minor changes as previously described (Carrocci et al. 2017). IR700 dye conjugated probes (Integrated DNA Technologies) were used for primer extension of the ACT1–CUP1 reporter (10 pmol yAC6: /5IRD700/GGCACTCATGACCTTC) and U6 snRNA (2 pmol yU6: /5IRD700/GAACTGCTGATCATGTCTG) (Carrocci et al. 2017; van der Feltz et al. 2021). Primer extension products were visualized on a 7% (w/v) denaturing polyacrylamide gel (42 cm × 22 cm × 0.75 mm) run at 35W for 80 min at RT. Gels were imaged with an Amersham Typhoon NIR laser scanner (Cytiva), and band intensities were quantified with ImageJ (v1.53, 2022).

RT-PCR

Cell cultures were inoculated from stationary phase saturated cultures grown overnight in YPD media. The cultures were then grown until $OD_{600} = 0.7–0.9$, and 1 mL of cells was collected by centrifugation. Total RNA was isolated from yeast, and contaminating DNA was depleted using the MasterPure Yeast RNA Purification Kit (Epicentre) protocol with minor changes as previously described (Carrocci et al. 2017). RT-PCR reactions were set up using the Access RT-PCR System (Promega Corporation) protocol with 75 ng RNA per 25 µL reaction. Primers used were SUS1-exon1 5′-TGGATACTGCGCAATTAAAGAGTC-3′ and SUS1-exon3 5′-TCATTGTGTATCTACAATCTCTTCAAG-3′. Products of the reaction were run on 2% (w/v) agarose-TBE gels and imaged. Band intensities were quantified with ImageJ Software (v1.53, 2022) (Schindelin et al. 2015). In order to identify the sequences of the reaction products, TOPO cloning (TOPO TA Cloning Kit, Thermo Fisher) was used to insert the RT-PCR products into a vector, and the inserts were then Sanger sequenced.

Splicing assays

Splicing WCEs and [^{32}P]-labeled RP51A substrate pre-mRNAs were prepared as previously described (Crawford et al. 2008). Splicing assays were conducted at room temperature using 40% (v/v) WCE and 0.2 nM pre-mRNA substrate (Crawford et al. 2008). [^{32}P]-labeled RNAs were then isolated and separated on a 12% (w/v) denaturing PAGE gel followed by phosphor imaging after exposing gels overnight to the phosphor imaging screen. Data were analyzed using ImageJ. The fractions of the lariat intermediate and efficiencies of the second step were calculated using Equations 1 and 2 and the corresponding band intensities as previously described (Mayerle and Guthrie 2016).

$$\text{Fraction lariat intermediate} = \frac{\text{lariat intermediate}}{\text{pre-mRNA} + \text{lariat intermediate} + \text{mRNA}} \quad (1)$$

$$\text{Second-step efficiency} = \frac{\text{mRNA}}{\text{lariat intermediate} + \text{mRNA}} \quad (2)$$

SUPPLEMENTAL MATERIAL

Supplemental material is available for this article.

COMPETING INTEREST STATEMENT

A.A.H. is a member of the scientific advisory board and is carrying out sponsored research for Remix Therapeutics.

ACKNOWLEDGMENTS

We thank Guilaume Chanfreau and his laboratory for helpful discussions and critical review of the manuscript. We thank Peter Ducos and Tim Grant for assistance in making Figure 1. This work was supported by grants from the National Institutes of Health (R35 GM136261 to A.A.H.), the NIH Biotechnology Training Program (T32 GM135066), and the National Science Foundation Graduate Research Fellowship Program (grant no. DGE-1747503) fellowships to K.A.S.

Received January 30, 2023; accepted August 4, 2023.

REFERENCES

Auesukaree C, Damnernsawad A, Kruatrachue M, Pokethitiyook P, Boonchird C, Kaneko Y, Harashima S. 2009. Genome-wide identification of genes involved in tolerance to various environmental stresses in *Saccharomyces cerevisiae*. *J Appl Genet* **50:** 301–310. doi:10.1007/BF03195688

Bastian M, Heymann S, Jacomy M. 2009. Gephi: an open source software for exploring and manipulating networks. *Proc Int AAAI Conf Web Soc Media* **3:** 361–362. doi:10.1609/icwsm.v3i1.13937

Brys A, Schwer B. 1996. Requirement for SLU7 in yeast pre-mRNA splicing is dictated by the distance between the branchpoint and the 3′ splice site. *RNA* **2:** 707–717.

Carrocci TJ, Zoerner DM, Paulson JC, Hoskins AA. 2017. SF3b1 mutations associated with myelodysplastic syndromes alter the fidelity of branchsite selection in yeast. *Nucleic Acids Res* **45:** 4837–4852. doi:10.1093/nar/gkw1349

Carrocci TJ, Paulson JC, Hoskins AA. 2018. Functional analysis of Hsh155/SF3b1 interactions with the U2 snRNA/branch site duplex. *RNA* **24:** 1028–1040. doi:10.1261/rna.065664.118

Chiu Y-F, Liu Y-C, Chiang T-W, Yeh T-C, Tseng C-K, Wu N-Y, Cheng S-C. 2009. Cwc25 is a novel splicing factor required after Prp2 and Yju2 to facilitate the first catalytic reaction. *Mol Cell Biol* **29:** 5671–5678. doi:10.1128/MCB.00773-09

Crawford DJ, Hoskins AA, Friedman LJ, Gelles J, Moore MJ. 2008. Visualizing the splicing of single pre-mRNA molecules in whole cell extract. *RNA* **14:** 170–179. doi:10.1261/rna.794808

Crotti LB, Bačíková D, Horowitz DS. 2007. The Prp18 protein stabilizes the interaction of both exons with the U5 snRNA during the second step of pre-mRNA splicing. *Genes Dev* **21:** 1204–1216. doi:10.1101/gad.1538207

Cuenca-Bono B, García-Molinero V, Pascual-García P, Dopazo H, Llopis A, Vilardell J, Rodríguez-Navarro S. 2011. *SUS1* introns are required for efficient mRNA nuclear export in yeast. *Nucleic Acids Res* **39:** 8599–8611. doi:10.1093/nar/gkr496

Eysmont K, Matylla-Kulińska K, Jaskulska A, Magnus M, Konarska MM. 2019. Rearrangements within the U6 snRNA core during the transition between the two catalytic steps of splicing. *Mol Cell* **75:** 538–548.e3. doi:10.1016/j.molcel.2019.05.018

Fabrizio P, Dannenberg J, Dube P, Kastner B, Stark H, Urlaub H, Lührmann R. 2009. The evolutionarily conserved core design of the catalytic activation step of the yeast spliceosome. *Mol Cell* **36:** 593–608. doi:10.1016/j.molcel.2009.09.040

Fica SM, Nagai K. 2017. Cryo-electron microscopy snapshots of the spliceosome: structural insights into a dynamic ribonucleoprotein machine. *Nat Struct Mol Biol* **24:** 791–799. doi:10.1038/nsmb.3463

Fica SM, Oubridge C, Galej WP, Wilkinson ME, Bai X-C, Newman AJ, Nagai K. 2017. Structure of a spliceosome remodelled for exon ligation. *Nature* **542:** 377–380. doi:10.1038/nature21078

Frank D, Guthrie C. 1992. An essential splicing factor, *SLU7*, mediates 3′ splice site choice in yeast. *Genes Dev* **6:** 2112–2124. doi:10.1101/gad.6.11.2112

Goldstein AL, McCusker JH. 1999. Three new dominant drug resistance cassettes for gene disruption in *Saccharomyces cerevisiae*. *Yeast* **15:** 1541–1553. doi:10.1002/(SICI)1097-0061(199910)15:14<1541::AID-YEA476>3.0.CO;2-K

Hossain MA, Claggett JM, Nguyen T, Johnson TL. 2009. The cap binding complex influences H2B ubiquitination by facilitating splicing of the SUS1 pre-mRNA. *RNA* **15:** 1515–1527. doi:10.1261/rna.1540409

Hossain MA, Rodriguez CM, Johnson TL. 2011. Key features of the two-intron *Saccharomyces cerevisiae* gene SUS1 contribute to its alternative splicing. *Nucleic Acids Res* **39:** 8612–8627. doi:10.1093/nar/gkr497

Hotz H-R, Schwer B. 1998. Mutational analysis of the yeast DEAH-box splicing factor Prp16. *Genetics* **149:** 807–815. doi:10.1093/genetics/149.2.807

Huh W-K, Falvo JV, Gerke LC, Carroll AS, Howson RW, Weissman JS, O'Shea EK. 2003. Global analysis of protein localization in budding yeast. *Nature* **425:** 686–691. doi:10.1038/nature02026

James S-A, Turner W, Schwer B. 2002. How Slu7 and Prp18 cooperate in the second step of yeast pre-mRNA splicing. *RNA* **8:** 1068–1077. doi:10.1017/s1355838202022033

Jonik-Nowak B, Menneteau T, Fesquet D, Baldin V, Bonne-Andrea C, Méchali F, Fabre B, Boisguerin P, de Rossi S, Henriquet C, et al. 2018. PIP30/FAM192A is a novel regulator of the nuclear proteasome activator PA28γ. *Proc Natl Acad Sci* **115:** E6477–E6486. doi:10.1073/pnas.1722299115

Jumper J, Evans R, Pritzel A, Green T, Figurnov M, Ronneberger O, Tunyasuvunakool K, Bates R, Žídek A, Potapenko A, et al. 2021. Highly accurate protein structure prediction with AlphaFold. *Nature* **596:** 583–589. doi:10.1038/s41586-021-03819-2

Kao CY, Cao EC, Wai HL, Cheng SC. 2021. Evidence for complex dynamics during U2 SnRNP selection of the intron branchpoint. *Nucleic Acids Res* **49:** 9965–9977. doi:10.1093/nar/gkab695

Kaur H, van der Feltz C, Sun Y, Hoskins AA. 2022. Network theory reveals principles of spliceosome structure and dynamics. *Structure* **30:** 190–200.e2. doi:10.1016/j.str.2021.09.003

Kawashima T, Pellegrini M, Chanfreau GF. 2009. Nonsense-mediated mRNA decay mutes the splicing defects of spliceosome component mutations. *RNA* **15:** 2236–2247. doi:10.1261/rna.1736809

Kawashima T, Douglass S, Gabunilas J, Pellegrini M, Chanfreau GF. 2014. Widespread use of non-productive alternative splice sites in *Saccharomyces cerevisiae*. *PLoS Genet* **10:** e1004249. doi:10.1371/journal.pgen.1004249

Lesser CF, Guthrie C. 1993. Mutational analysis of pre-mRNA splicing in *Saccharomyces cerevisiae* using a sensitive new reporter gene, CUP1. *Genetics* **133:** 851–863. doi:10.1093/genetics/133.4.851

Liu Y-C, Chen H-C, Wu N-Y, Cheng S-C. 2007a. A novel splicing factor, Yju2, is associated with NTC and acts after Prp2 in promoting the first catalytic reaction of pre-mRNA splicing. *Mol Cell Biol* **27:** 5403–5413. doi:10.1128/MCB.00346-07

Liu L, Query CC, Konarska MM. 2007b. Opposing classes of prp8 alleles modulate the transition between the catalytic steps of pre-mRNA splicing. *Nat Struct Mol Biol* **14:** 519–526. doi:10.1038/nsmb1240

Liu S, Li X, Zhang L, Jiang J, Hill RC, Cui Y, Hansen KC, Zhou ZH, Zhao R. 2017. Structure of the yeast spliceosomal postcatalytic P complex. *Science* **358:** 1278–1283. doi:10.1126/science.aar3462

Maitra N, Anandhakumar J, Blank HM, Kaplan CD, Polymenis M. 2019. Perturbations of transcription and gene expression-associated processes alter distribution of cell size values in *Saccharomyces cerevisiae*. *G3 (Bethesda)* **9:** 239–250. doi:10.1534/g3.118.200854

Mayerle M, Guthrie C. 2016. Prp8 retinitis pigmentosa mutants cause defects in the transition between the catalytic steps of splicing. *RNA* **22:** 793–809. doi:10.1261/rna.055459.115

Needleman SB, Wunsch CD. 1970. A general method applicable to the search for similarities in the amino acid sequence of two proteins. *J Mol Biol* **48:** 443–453. doi:10.1016/0022-2836(70)90057-4

Ohrt T, Odenwälder P, Dannenberg J, Prior M, Warkocki Z, Schmitzová J, Karaduman R, Gregor I, Enderlein J, Fabrizio P, et al. 2013. Molecular dissection of step 2 catalysis of yeast pre-mRNA splicing investigated in a purified system. *RNA* **19:** 902–915. doi:10.1261/rna.039024.113

Pagé N, Gérard-Vincent M, Ménard P, Beaulieu M, Azuma M, Dijkgraaf GJP, Li H, Marcoux J, Nguyen T, Dowse T, et al. 2003. A *Saccharomyces cerevisiae* genome-wide mutant screen for altered sensitivity to K1 killer toxin. *Genetics* **163:** 875–894. doi:10.1093/genetics/163.3.875

Pettersen EF, Goddard TD, Huang CC, Meng EC, Couch GS, Croll TI, Morris JH, Ferrin TE. 2021. UCSF ChimeraX: structure visualization for researchers, educators, and developers. *Protein Sci* **30:** 70–82. doi:10.1002/pro.3943

Plaschka C, Newman AJ, Nagai K. 2019. Structural basis of nuclear pre-mRNA splicing: lessons from yeast. *Cold Spring Harb Perspect Biol* **11:** a032391. doi:10.1101/cshperspect.a032391

Query CC, Konarska MM. 2004. Suppression of multiple substrate mutations by spliceosomal *prp8* alleles suggests functional correlations with ribosomal ambiguity mutants. *Mol Cell* **14:** 343–354. doi:10.1016/S1097-2765(04)00217-5

Query CC, Konarska MM. 2006. Splicing fidelity revisited. *Nat Struct Mol Biol* **13:** 472–474. doi:10.1038/nsmb0606-472

Query CC, Konarska MM. 2012. *CEF1/CDC5* alleles modulate transitions between catalytic conformations of the spliceosome. *RNA* **18:** 1001–1013. doi:10.1261/rna.029421.111

Sayani S, Janis M, Lee CY, Toesca I, Chanfreau GF. 2008. Widespread impact of nonsense-mediated mRNA decay on the yeast intronome. *Mol Cell* **31:** 360–370. doi:10.1016/j.molcel.2008.07.005

Schindelin J, Rueden CT, Hiner MC, Eliceiri KW. 2015. The ImageJ ecosystem: an open platform for biomedical image analysis. *Mol Reprod Dev* **82:** 518–529. doi:10.1002/mrd.22489

Schneider S, Campodonico E, Schwer B. 2004. Motifs IV and V in the DEAH box splicing factor Prp22 are important for RNA unwinding, and helicase-defective Prp22 mutants are suppressed by Prp8. *J Biol Chem* **279:** 8617–8626. doi:10.1074/jbc.M312715200

Schwer B. 2008. A conformational rearrangement in the spliceosome sets the stage for Prp22-dependent mRNA release. *Mol Cell* **30:** 743–754. doi:10.1016/j.molcel.2008.05.003

Schwer B, Gross CH. 1998. Prp22, a DExH-box RNA helicase, plays two distinct roles in yeast pre-mRNA splicing. *EMBO J* **17:** 2086–2094. doi:10.1093/emboj/17.7.2086

Schwer B, Guthrie C. 1992. A conformational rearrangement in the spliceosome is dependent on PRP16 and ATP hydrolysis. *EMBO J* **11:** 5033–5039. doi:10.1002/j.1460-2075.1992.tb05610.x

Schwer B, Meszaros T. 2000. RNA helicase dynamics in pre-mRNA splicing. *EMBO J* **19:** 6582–6591. doi:10.1093/emboj/19.23.6582

Semlow DR, Blanco MR, Walter NG, Staley JP. 2016. Spliceosomal DEAH-Box ATPases remodel pre-mRNA to activate alternative splice sites. *Cell* **164:** 985–998. doi:10.1016/j.cell.2016.01.025

Sikorski RS, Boeke JD. 1991. *In vitro* mutagenesis and plasmid shuffling: from cloned gene to mutant yeast. *Methods Enzymol* **194:** 302–318. doi:10.1016/0076-6879(91)94023-6

Treco DA, Lundblad V. 1993. Preparation of yeast media. *Curr Protoc Mol Biol* **23:** 13.1.1–13.1.7. doi:10.1002/0471142727.mb1301s23

Umen JG, Guthrie C. 1995a. A novel role for a U5 snRNP protein in 3′ splice site selection. *Genes Dev* **9:** 855–868. doi:10.1101/gad.9.7.855

Umen JG, Guthrie C. 1995b. Prp16p, Slu7p, and Prp8p interact with the 3′ splice site in two distinct stages during the second catalytic step of pre-mRNA splicing. *RNA* **1:** 584–597.

van der Feltz C, Nikolai B, Schneider C, Paulson JC, Fu X, Hoskins AA. 2021. *Saccharomyces cerevisiae* Ecm2 modulates the catalytic steps of pre-mRNA splicing. *RNA* **27:** 591–603. doi:10.1261/rna.077727.120

Viladevall L, Serrano R, Ruiz A, Domenech G, Giraldo J, Barceló A, Ariño J. 2004. Characterization of the calcium-mediated response to alkaline stress in *Saccharomyces cerevisiae*. *J Biol Chem* **279:** 43614–43624. doi:10.1074/jbc.M403606200

Villa T, Guthrie C. 2005. The Isy1p component of the NineTeen complex interacts with the ATPase Prp16p to regulate the fidelity of pre-mRNA splicing. *Genes Dev* **19:** 1894–1904. doi:10.1101/gad.1336305

Wagner JDO, Jankowsky E, Company M, Pyle AM, Abelson JN. 1998. The DEAH-box protein PRP22 is an ATPase that mediates ATP-dependent mRNA release from the spliceosome and unwinds RNA duplexes. *EMBO J* **17:** 2926–2937. doi:10.1093/emboj/17.10.2926

Wan R, Bai R, Yan C, Lei J, Shi Y. 2019. Structures of the catalytically activated yeast spliceosome reveal the mechanism of branching. *Cell* **177:** 339–351.e13. doi:10.1016/j.cell.2019.02.006

Warkocki Z, Odenwälder P, Schmitzová J, Platzmann F, Stark H, Urlaub H, Ficner R, Fabrizio P, Lührmann R. 2009. Reconstitution of both steps of *Saccharomyces cerevisiae* splicing with purified spliceosomal components. *Nat Struct Mol Biol* **16:** 1237–1243. doi:10.1038/nsmb.1729

Wilkinson ME, Fica SM, Galej WP, Norman CM, Newman AJ, Nagai K. 2017. Post-catalytic spliceosome structure reveals mechanism of 3′-splice site selection. *Science* **358:** 1283–1288. doi:10.1126/science.aar3729

Wilkinson ME, Fica SM, Galej WP, Nagai K. 2021. Structural basis for conformational equilibrium of the catalytic spliceosome. *Mol Cell* **81:** 1439–1452.e9. doi:10.1016/j.molcel.2021.02.021

Wilson TE. 2002. A genomics-based screen for yeast mutants with an altered recombination/end-joining repair ratio. *Genetics* **162:** 677–688. doi:10.1093/genetics/162.2.677

Yan C, Wan R, Bai R, Huang G, Shi Y. 2017. Structure of a yeast step II catalytically activated spliceosome. *Science* **355:** 149–155. doi:10.1126/science.aak9979

Zhan X, Lu Y, Zhang X, Yan C, Shi Y. 2022. Mechanism of exon ligation by human spliceosome. *Mol Cell* **82:** 2769–2778.e4. doi:10.1016/j.molcel.2022.05.021

See the following page for ***Meet the First Authors***

MEET THE FIRST AUTHORS

Katherine Senn

Karli Lipinski

***Meet the First Author(s)* is an editorial feature within *RNA*, in which the first author(s) of research-based papers in each issue have the opportunity to introduce themselves and their work to readers of *RNA* and the RNA research community. Katherine Senn and Karli Lipinski are joint first authors of this paper, "Biochemical and genetic evidence supports Fyv6 as a second-step splicing factor in *Saccharomyces cerevisiae*." Katherine is a graduate student in the Integrated Program in Biochemistry whereas Karli is in the Chemistry graduate program, at the University of Wisconsin-Madison. They both are part of the Hoskins laboratory and work on the mechanism of pre-mRNA splicing.**

What are the major results described in your paper and how do they impact this branch of the field?

In this paper, we show for the first time that the protein Fyv6 is involved in pre-mRNA splicing in yeast. Deletion of *FYV6* has genetic interactions with other spliceosomal proteins and decreases splicing efficiency at the second step. Absence of the protein also alters 3′ splice site choice of a reporter gene and an endogenous gene. This biochemical and genetic evidence builds on the ambiguous structural evidence that suggested Fyv6 could be involved in splicing and identifies the protein as a novel splicing factor.

What led you to study RNA or this aspect of RNA science?

KS: I am broadly interested in the way regulation of gene expression can affect outcomes for and properties of a cell. There are different layers of this regulation at the RNA level, including pre-mRNA splicing, and the complexities of the spliceosome and associated factors in regulating and carrying out the splicing reaction make it an interesting process to study. This project has been a great opportunity to explore how a new splicing factor, Fyv6, fits in with the rest of the spliceosome to regulate splicing and help it progress correctly.

KL: The spliceosome is a very interesting RNP machine where the RNA coordinates the selection of splice sites and also performs the catalysis. Both functions can be modulated by the presence or absence of various protein components during the splicing cycle. It was exciting to have the opportunity to characterize a protein recently associated with splicing where very little was known about its function when we started our work.

During the course of these experiments, were there any surprising results or particular difficulties that altered your thinking and subsequent focus?

We were highly skeptical at the start of this project that Fyv6 was indeed a splicing factor from the inconclusive evidence available to us, which quickly evaporated as we completed the first few sets of experiments. The absence of Fyv6 results in marked changes in splicing and dramatic changes in growth. It was very exciting and suddenly we had many more questions we wanted to explore, some of which are answered here and some are saved for future work.

What are some of the landmark moments that provoked your interest in science or your development as a scientist?

KS: While I enjoyed learning about science throughout my schooling, there was one experience in high school that made me seriously begin to think about a career related to scientific research. In my AP Biology class, each student had to complete an independent research project. I was able to design and carry out an experiment that interested me, and which did not already have a clearly defined expected result like other labs in which I'd worked up to that point. The experience made me realize that I liked the process of research and finding answers to questions that were of interest and importance to me and others in the world.

KL: I was a summer research student in the laboratory of Dr. Grover Miller at UAMS College of Medicine prior to my junior year of college. Dr. Miller is passionate about mentoring undergraduate students and took great care to teach me the best practices for scientific communication during my brief stay in his laboratory. I gave my first scientific research presentation on work from his laboratory to a room of 200+ people while feeling prepared and confident. I can trace the great successes I have had with and the joy I have in communicating science back to this moment.

What are your subsequent near- or long-term career plans

KS: I will be wrapping up my graduate work in the near future. From there, I plan to find a job in industry, potentially continuing to work in an RNA-related field. I would love to continue to contribute to scientific advances by focusing on research and development.

KL: I will also be completing my doctorate degree soon and plan to look for a postdoctoral position in RNA biology broadly. I want to continue to inspire and train the next generation of scientists while answering fundamental questions to further our understanding of RNA processes within cells.